extra 2nd Report

NASA CR-54025
EOS Report 4920-Q-1

dtd 6/20/64

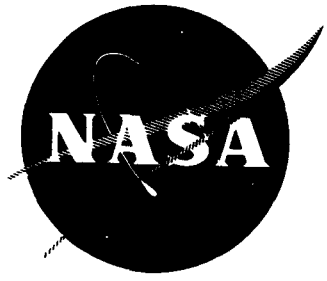

ION ROCKET SYSTEM RESEARCH AND DEVELOPMENT

by

G. Sohl, G. C. Reid, and R. C. Speiser

prepared for

NATIONAL AERONAUTICS AND SPACE ADMINISTRATION

CONTRACT NAS3-5250

EOS ELECTRO-OPTICAL SYSTEMS, INC., PASADENA, CALIFORNIA

Requests for copies of this report should be referred to

National Aeronautics and Space Administration
Office of Scientific and Technical Information
Attention: AFSS-A
Washington, D.C. 20546

NASA CR-54025
EOS Report 4920-Q-1

QUARTERLY REPORT

ION ROCKET SYSTEM RESEARCH AND DEVELOPMENT

by

G. Sohl, G. C. Reid, and R. C. Speiser

prepared for

NATIONAL AERONAUTICS AND SPACE ADMINISTRATION

20 June 1964

CONTRACT NAS3-5250

Technical Management
NASA Lewis Research Center
Cleveland, Ohio
Spacecraft Technology Division
James Wolters

ELECTRO-OPTICAL SYSTEMS, INC.
300 No. Halstead Street
Pasadena, California

ABSTRACT

Work performed in the first quarter of a research and development program on an electron bombardment cesium ion rocket system is reported. The facility for extended testing of the system and some initial tests are described. The performance of a permanent magnet version of the engine is reported and the results of plasma distribution studies and autocathode improvement tests are discussed.

TABLE OF CONTENTS

ILLUSTRATIONS

SUMMARY

This quarterly report for the period 24 February 1964 to 31 May 1964 describes the work performed under Contract NAS3-5250. The objectives of the program are to continue the development and testing of the engine and feed system developed under Contract NAS3-2516; to investigate the use of permanent magnets with the electron bombardment cesium ion engine; to study the plasma distribution in electron bombardment cesium ion sources; and to make improvements in the cesiated autocathodes used in the engines.

During the report period a facility for extended testing of the engine and feed system was built and tests were begun. A permanent magnet modification of the engine was fabricated and it was determined that engine operation was as good as with electromagnets. The ion and neutral efflux distributions from an engine were determined for different operating conditions and for different cesium injection geometries. Starting power requirements for the autocathode were investigated and a new cathode with no internal heater was fabricated and tested.

The main conclusions from the results obtained in the first quarter are that a lightweight permanent magnet engine design is feasible and that the starting power requirements of the autocathode can be greatly reduced. It appears that some of the neutral efflux from an engine is due to evaporation of cesium directly from the anode and a change in the anode design might increase the mass utilization efficiency with no increase in arc power.

1. INTRODUCTION

This is the first Quarterly Report under Contract NAS3-5250, ION ROCKET SYSTEM RESEARCH AND DEVELOPMENT. The program is a follow-on to the completed contract NAS3-2516 and is based partly on the continued development and testing of the DE engine system developed under that contract and reported in EOS Report 3670-Final, "Ion Rocket Engine System Research and Development", (NASA CR-54067). The 3 kw system (designated DE) developed on Contract NAS3-2516 is composed of a 10 mlb. engine with zero-g feed system and a laboratory control system which provides automatic start-ups and shut-downs and handles transients.

1.1 Program Objectives

The present program provides for the continued development and testing of the DE engine and feed system to achieve demonstrated long life and reliability. It includes the elimination of short and long term failure modes and the evaluation of lifetime limitations. A quality assurance and reliability program is being followed on this task.

In addition to the long-life engine and feed system program, three research and development programs are being pursued. They are:

1. Design, fabrication, and testing of a permanent magnet version of the DE engine.
2. Plasma distribution studies to investigate basic means of improving engine operation and lifetime.
3. Autocathode improvement studies to reduce the starting power requirements of cesium electron bombardment ion engines.

1.2 Key Personnel

The key personnel on the program, and their areas of effort, are:

R. C. Speiser	Program Supervisor
G. C. Reid	Long Life Engine
F. A. Barcatta	Long Life Feed System
G. Sohl	Applied Research
S. Zafran	Quality Assurance

These personnel supervise their respective tasks and are the major contributors to the program and to all reports generated under the program.

1.3 General Status

During the quarter, a test facility for lifetime and reliability testing of the DE engine and feed system was prepared and initial testing was begun. A permanent magnet modification of the DE engine was fabricated and operated and its performance was comparable to that of the electromagnet engine.

Plasma distribution studies were undertaken and ion and neutral efflux distributions from a bombardment engine were determined. The effects of the magnetic field intensity and cathode orifice configuration on the ion and neutral efflux distributions were investigated. The performance of the DE engine using different cathode orifice sizes was investigated and minimum autocathode starting temperatures were determined. Start-ups were made without using the internal cathode heater and an autocathode configuration with no internal heater was designed, fabricated, and tested.

2. LONG LIFE ENGINE

2.1 Facility

Figure 1 is a schematic of the test chamber which was prepared for reliability testing of the DE engine and feed system. The engine is mounted in a tank section 28 inches in diameter and 3-1/2 ft. long. This section has a 2 foot diameter liquid nitrogen cooled liner and is pumped by a 10 inch diffusion pump with a 6 inch standby pump. Both pumps have liquid nitrogen cooled baffles. This section has a neutral cesium detector with a housing which is cooled by conduction to the liner. The detector has a mechanically operated shutter for determining background levels.

The collector section of the facility is 28 inches in diameter and 5 feet long. It has a 2 foot diameter liquid nitrogen cooled liner with baffles cooled by conduction. The collector is made of heavy stacked copper plates and is water cooled. Liquid nitrogen is run through the diffusion pump baffle, the collector section liner and the engine section liner in that order and flow is controlled to regulate the outlet temperature of the engine section liner. The collector and both liner sections can be floated for neutralization tests.

The engine and feed system are operated by a DE control system of the type discussed in EOS Report 3670-Final (NASA CR-54067). Vacuum, power, and high voltage functions are interlocked to provide alarm signals or shut the system down in the event of engine system or test equipment malfunctions.

2.2 DER-1 Engine

Figure 2 is a photograph of the first engine and feed system assembled for the test program. It differs from the system tested under Contract 3-2516 only in the configuration of the shield in front of the accelerating electrode and the positioning of thermocouples and power leads. This first assembly had a copper accelerating electrode, instead of molybdenum, to obtain erosion data in short duration runs.

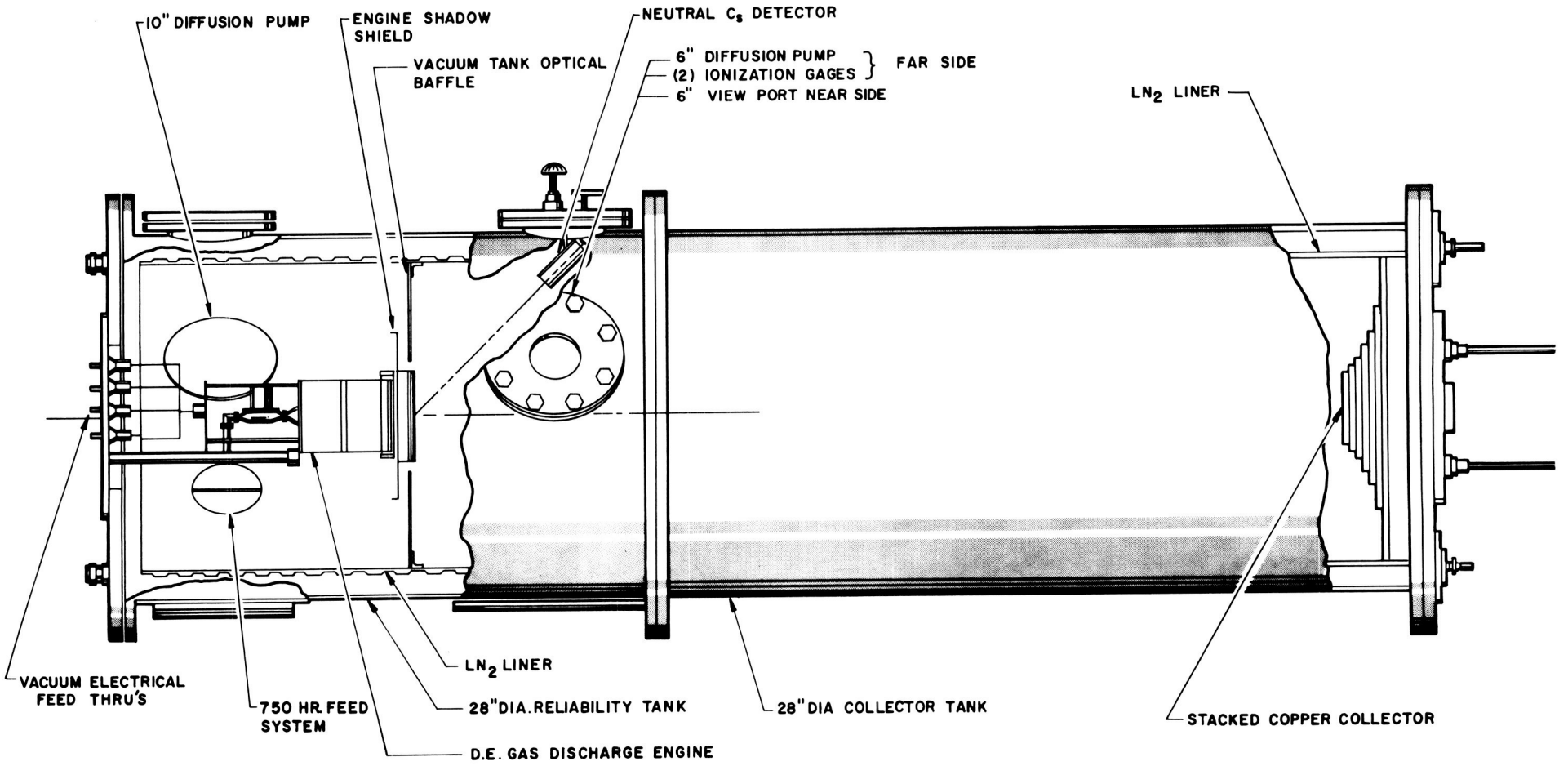

FIG. 1 DE ENGINE RELIABILITY SYSTEM

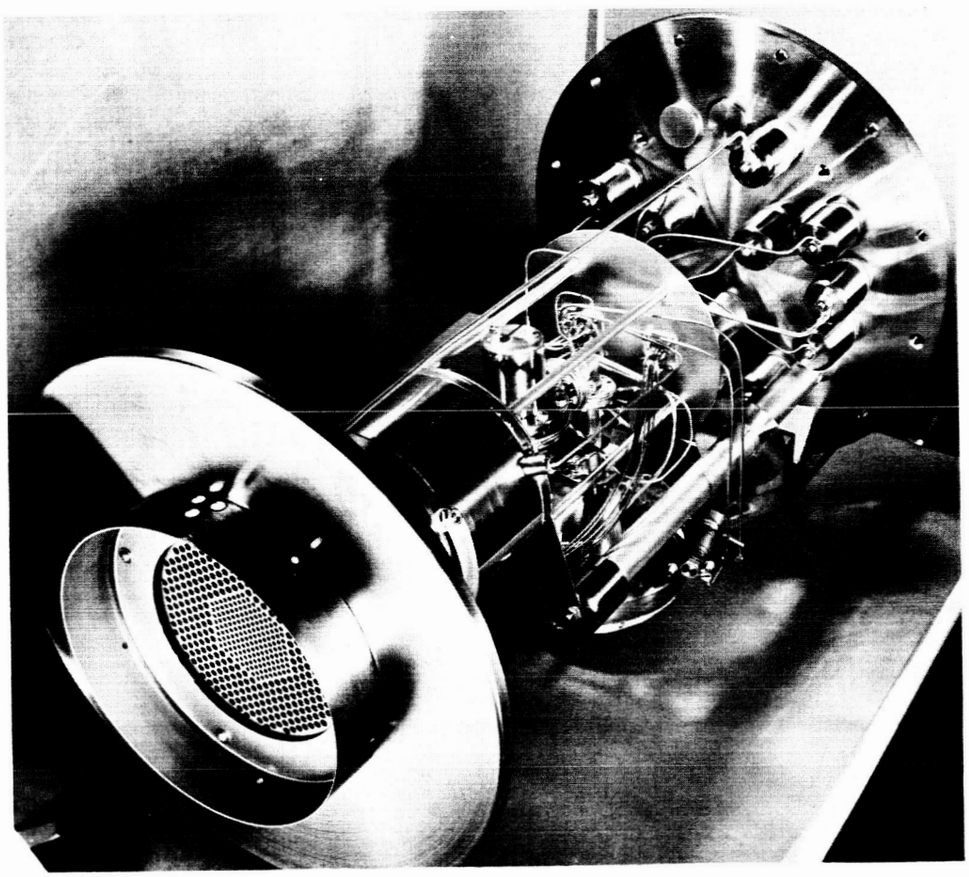

FIG. 2 DER-1 ENGINE

Table I lists component and sub-assembly weights for the DER-1 engine. All weights were taken with clean parts prior to operation of the engine.

TABLE I

ENGINE COMPONENT WEIGHTS

Component	Part No.	Weight	Accuracy
Screen electrode	703741B	118.7096 gm	±.0001 gm
Accelerator (Mo)	703714B	161.7473 gm	±.0001 gm
Accelerator (Cu)	703714B (SK394)	141.0190 gm	±.0001 gm
Electrode Support	703712	46.47335 gm	±.00005 gm
Hood	703758	116.0482 gm	±.0002 gm
Electrode Assembly	703705 (SK406)	483.4964 gm	±.0002 gm
Anode	703711A	353.95 gm	±.05 gm
Cathode Assembly	703709V	100.1301 gm	±.0001 gm
Cathode Plate	703729B-2	135.4041 gm	±.0001 gm
Shell Assembly	703708C	748.15 gm	±.05 gm

2.3 Initial Tests

2.3.1 Initial Engine Operation

The initial check-out test of the DER-1 engine was made using the copper acceleration electrode. Performance was as expected with operating parameters as listed in Table II. The run was terminated after a total accumulated time of 9 hours due to a leak in the liquid nitrogen cooling line of the collector (the initial test was made in another facility since the equipment of Figure 1 was not yet ready).

TABLE II

OPERATING PARAMETERS DURING INITIAL TEST

Positive High Voltage, V_+ (kv)	3.56
Negative High Voltage, V_- (kv)	0.76
Negative HV Current, I_- (amp)	0.0077
Beam Current, I_B (amp)	0.435
Arc Voltage, V_A (volt)	7.6
Arc Current, I_A (amp)	40.5
Beam Power, P_B (kw)	1.549
Drain Power, P_D (kw)	0.033
Magnet Power, P_M (kw)	0.010
Arc Power, P_A (kw)	0.308
Total Power, P_T (kw)	1.900
Thrust, T (mlb)	9.75
Power to Thrust, P/T (kw/lb)	195
Power Efficiency, η_p (percent)	80 %
Mass Efficiency, η_M (percent)	88 %
Overall Engine Efficiency, η_E (percent)	70.4 %
Specific Impulse I_{sp} (sec)	6440
I_-/I_B (percent)	1.8 %
P_A/I_B (kev/ion)	0.709

After the 9 hours of accumulated operation, the copper accelerating electrode was found to have lost 0.136 gm or 0.097 % of its weight. Erosion was evident between apertures on the downstream side of the electrode and was assumed to be due to charge exchange.

2.3.2 Engine System Tests

When the reliability test equipment was ready, the DER-1 engine, with a molybdenum accelerating electrode was mounted in the chamber and tests were started. Some trouble shooting of the test equipment was necessary during initial operation of the facility. The first run started normally and proceeded at operating levels similar to those of Table II. After 3-1/2 hours there was a malfunction of the high voltage power supplies which terminated the run. The cause was found to be intermittent arcs at a poor mechanical connection to the surge limiting resistors inside the positive high voltage power supply.

After the power supply was repaired, another run was started. After 1/2 hour at full beam (430 ma), the run was terminated due to inability to maintain high voltage. The engine was removed from the vacuum system and upon examination a black flaky substance was observed on the gap side of the accelerating electrode. This substance was also found in the arc chamber and on the liner under the electrode system.

Figure 3 shows a photograph of the electrode after the run. The foreign material appears as the dark coating and is heavier in the central region of the electrode. A sample of this substance was scraped from the plate and analyzed. The main constituents, by weight, were found to be:

Titanium	23 %
Copper	12 %
Aluminum	7 %
Nickel	4.1 %
Carbon	3.6 %
Molybdenum	2.9 %

Vanadium	2.6 %
Iron	1 %

The presence and high concentrations of titanium, aluminum, and vanadium indicate that some of the material may have come from the titanium alloy used for the cathode orifice plate. This alloy has the constituents:

Titanium	>89 %
Aluminum	6.1 %
Vanadium	4.1 %
Iron	0.17 %
Carbon	0.023 %

An examination of the orifice plate revealed severe distortion, indicating high temperatures around the orifice region. The orifice plate had lost 6.4 mg during the two tests which have been discussed. Figure 4 is a photograph of the orifice plate after the run. Usually, the whole plate is coated with copper sputtered back from the collector. The absence of copper over the central region indicates temperatures high enough to provide re-evaporation of deposited copper in this region. For the above reasons, it was decided that the foreign material was due to decomposition of the titanium alloy cathode orifice plate.

In the analysis of the flaky substance, the copper is assumed to be material sputtered back from the collector, the nickel to come from a braze used in assembling the cathode, and the molybdenum from the electrode itself.

A new cathode orifice plate of molybdenum will replace the titanium alloy part. Besides being a more refractory material, the molybdenum has higher thermal conductivity and will stay cooler than the titanium.

The engine was cleaned and reassembled and at the end of the quarter a third run was started, still using the titanium cathode orifice plate. This run was terminated after 23 hours due to high accelerator drain currents (25 ma). Analysis was not completed at the end

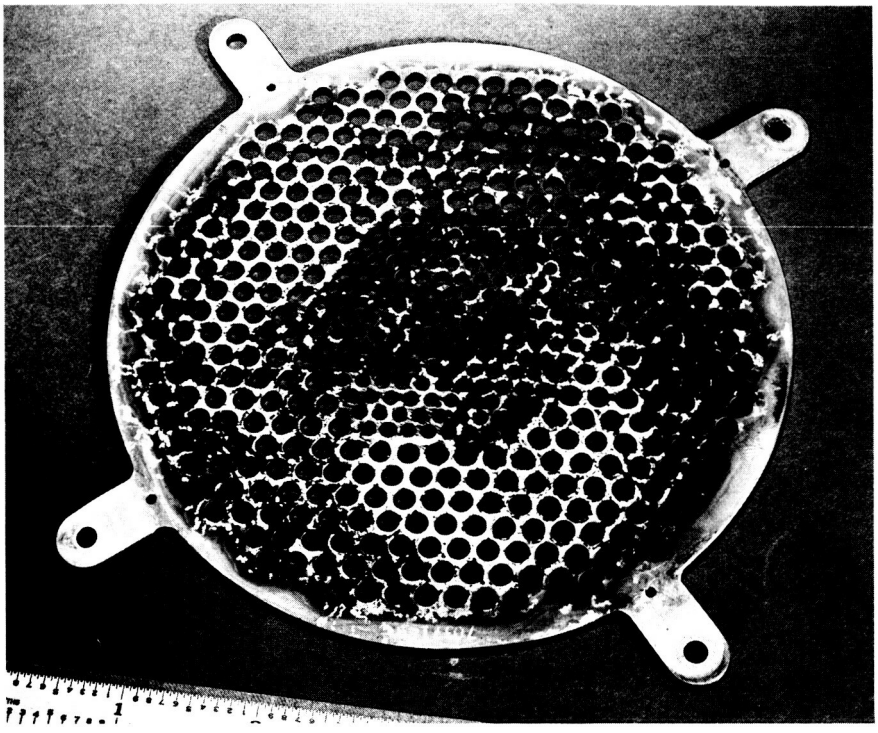

FIG. 3 DER-1 ACCELERATOR ELECTRODE
AFTER TEST

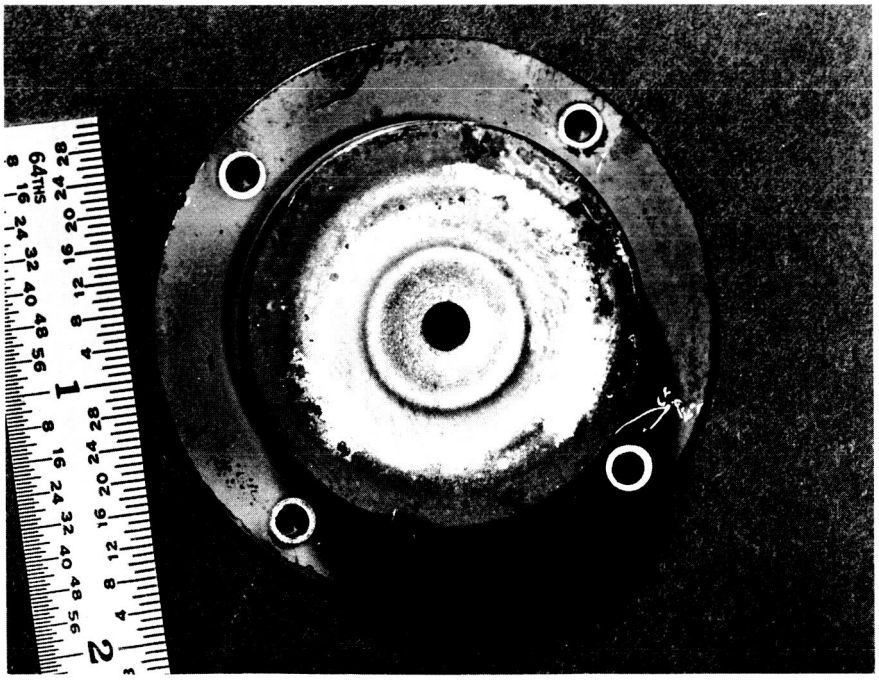

FIG. 4 DER-1 CATHODE ORIFICE PLATE
AFTER TEST

of the quarter.

3. PERMANENT MAGNET STUDIES

To reduce the power conditioning requirements of the engine and to reduce the system weight, if possible, the use of permanent magnets in the cesium electron bombardment ion engine is being investigated.

3.1 Magnetic Field

As a starting point in the design of a permanent magnet engine, the magnetic field of a DE engine was mapped. A plot of the axial field strength in gauss per ampere at three radial distances including the axis appears in Figure 5a. This plot served as a check on the experimental apparatus (a new engine shell and flux meter were used). The results were in good agreement with previous data obtained with the first two DE engine shells.

The radial field was also measured with the new apparatus and the data was reduced to yield the magnetic field plot shown in Figure 5b. As expected, the field was quite solenoidal. This plot was used as a reference for design of the permanent magnet field.

A permanent magnet modification of a basic DE engine was designed and built. For this first test, only the electromagnets, screen electrode, and cathode plate were modified. Pure iron was used as the permeable material. The modification was designed for operation with a number of rod shaped Alnico V permanent magnets. This was done to allow adjustment of the total cross section of the permanent magnet material by adding or removing magnets to obtain the desired field strength. The field, B, is determined by

$$B = \frac{B_R A_m}{K A_g}$$

where B_R is the residual flux density of the Alnico magnets, A_m is the cross sectional magnet area, A_g is the area of the gap (cathode to screen), and K is a form factor (approximately 4 for this circuit) which corrects for the effects of fringing. The demagnetizing force exerted on the

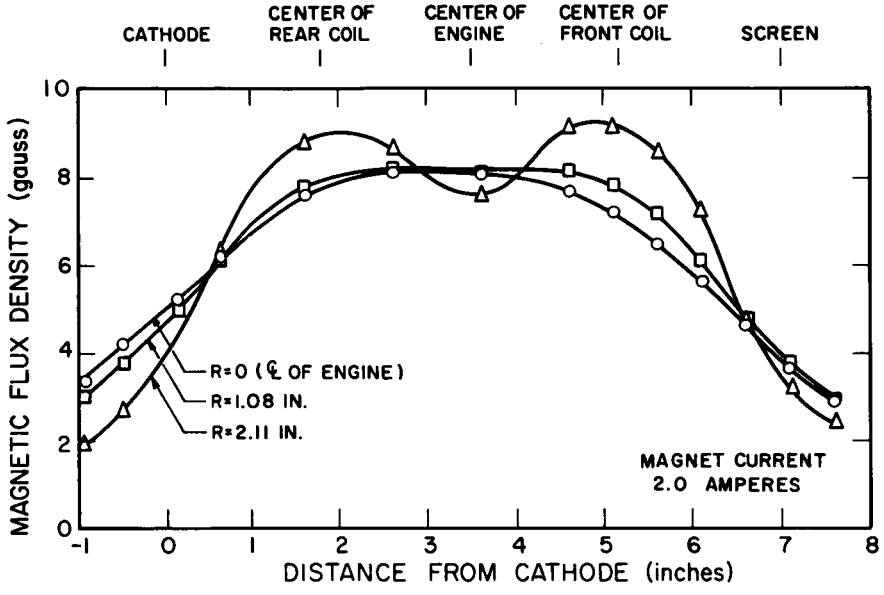

FIG. 5a AXIAL COMPONENT OF MAGNETIC FIELD OF DE ENGINE WITH ELECTROMAGNETS

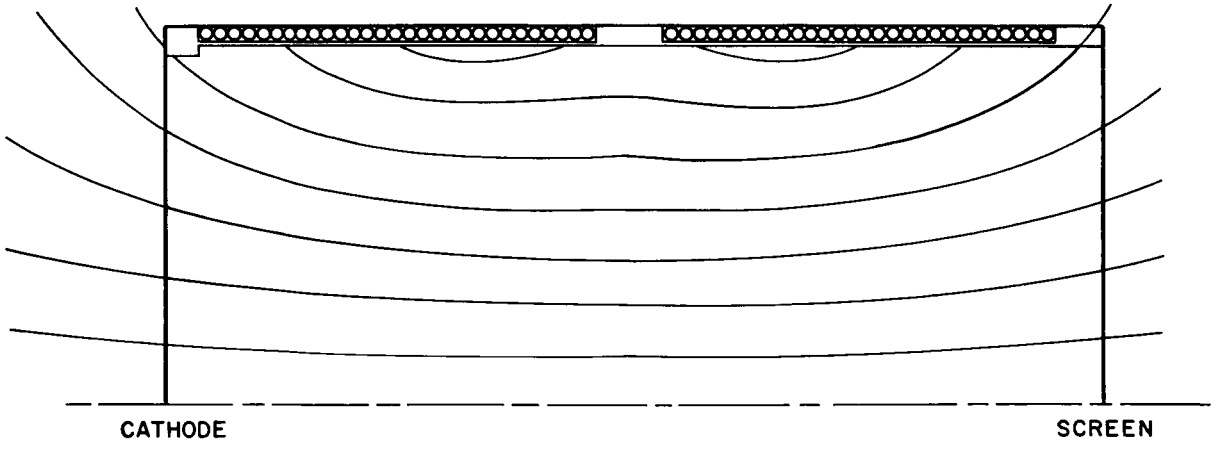

FIG. 5b PLOT OF MAGNETIC FIELD LINES FOR DE ENGINE WITH ELECTROMAGNETS

magnets in this configuration is only 10 oersteds at the desired field strength in the engine, which is not enough to reduce the flux in the Alnico magnets appreciably below B_R.

The field within the modified engine was measured and the number and size of the magnets were adjusted to obtain a field similar to that of the DE engine. Data on the axial component of the permanent magnet field are shown in Figure 6a. A clearer understanding of the differences may be obtained from Figures 5b and 6b. The convergence toward the screen electrode indicated in Figures 6a and 6b is due to the 15 percent larger area of the square cathode plate.

3.2 Engine Tests

The permanent magnet engine is shown in Figure 7. As can be seen, no attempt was made to keep this assembly small or light in weight. The engine, as modified, weighed two pounds more than the electromagnet version. Two thirds of this extra weight was in the cathode plate which was twice as thick as the screen electrode.

This modified engine was operated during the quarter with the following results:

1. Autocathode operation appeared satisfactory.
2. Some long period (several seconds) instabilities occurred at beam levels between 300 and 400 milliamperes. Beam fluctuations of 50 milliamperes were observed.
3. The modified screen electrode (Armco magnet iron) bowed toward the accelerating electrode enough to reduce the maximum voltage across the gap to 3.5 kilovolts during early operation.
4. Higher voltages could be sustained after preliminary operation.
5. Data taken at a 500 milliampere beam level are shown in Table III with similar data taken with the normal DE engine. The performance was comparable to that of the DE engine with the electromagnet configuration.

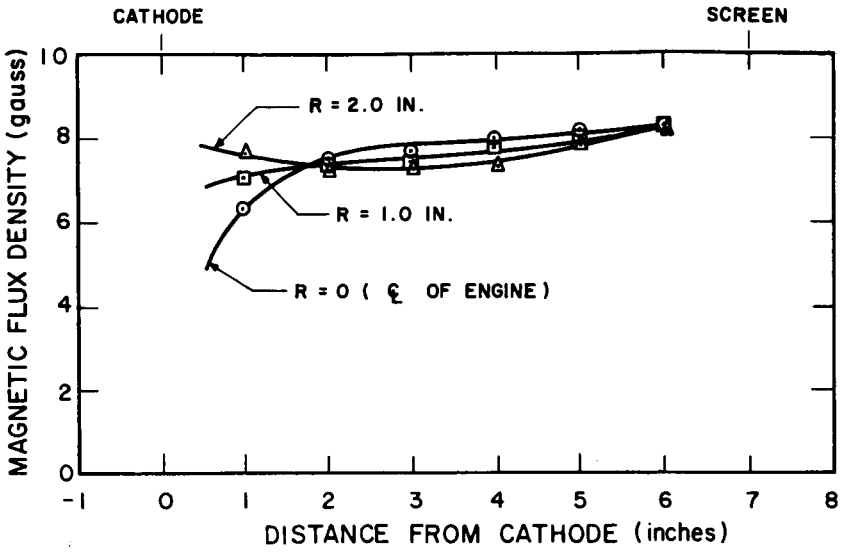

FIG. 6a AXIAL COMPONENT OF MAGNETIC FIELD OF DE ENGINE WITH PERMANENT MAGNETS

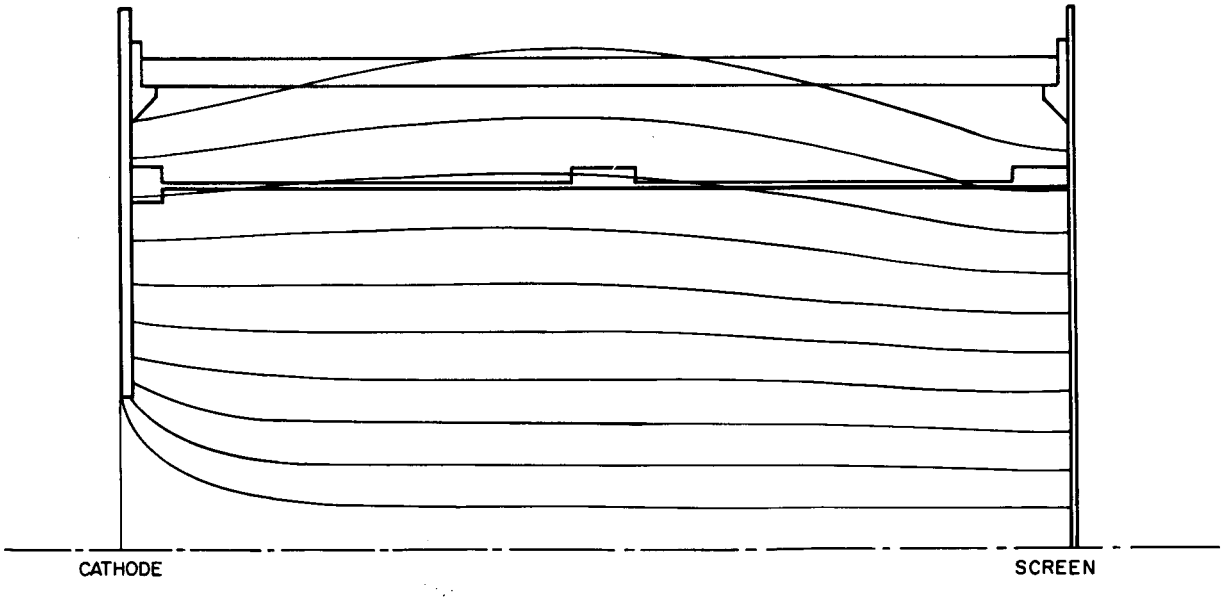

FIG. 6b PLOT OF MAGNETIC FIELD LINES FOR DE ENGINE WITH PERMANENT MAGNETS

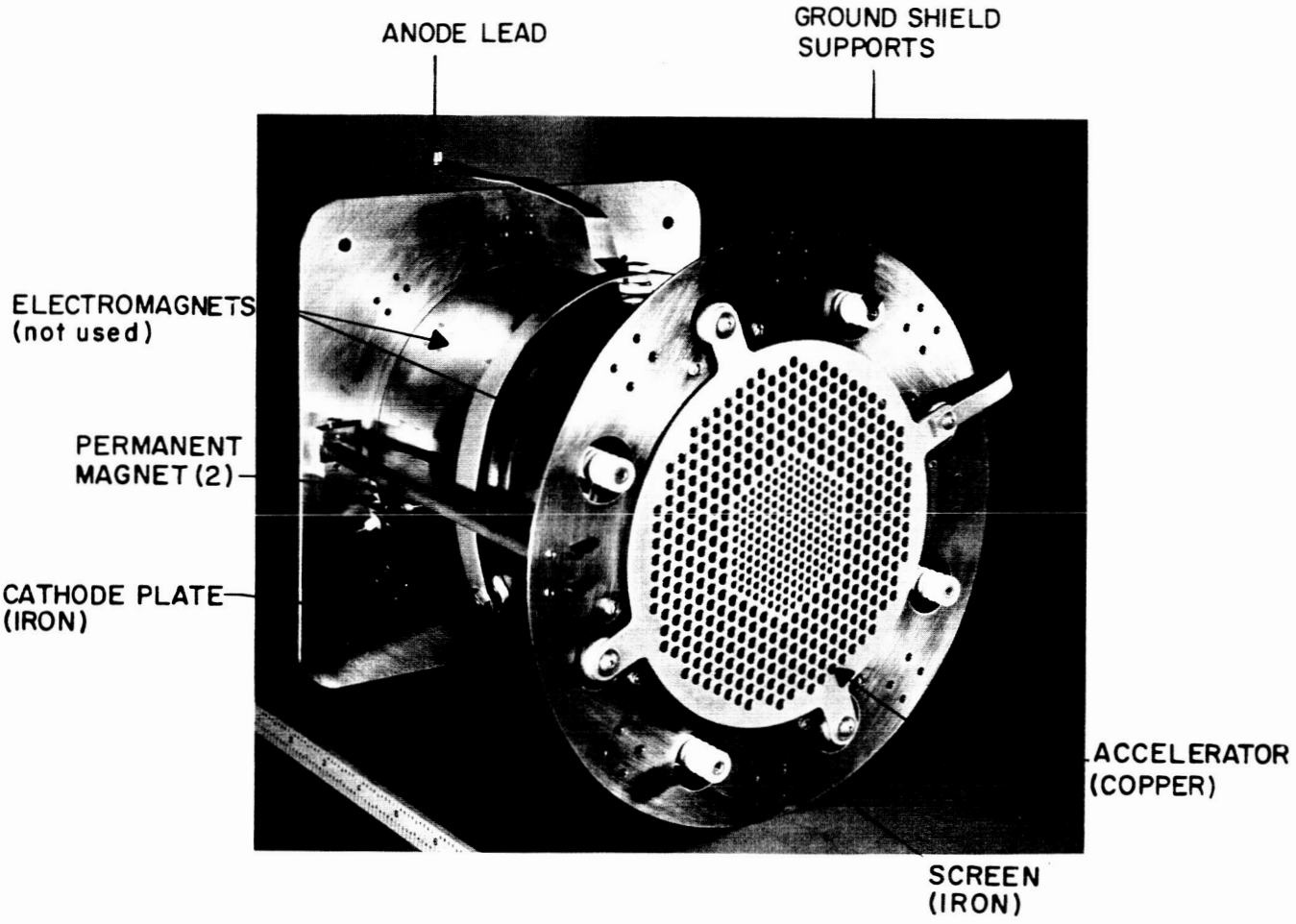

FIG. 7 DE ENGINE WITH PERMANENT MAGNET FIELD

TABLE III

COMPARISON OF DE ENGINE PERFORMANCE WITH ELECTROMAGNETS AND PERMANENT MAGNETS

	Electromagnets		Permanent Magnets
V_+(kv)	3.5	3.6	3.5
V_-(kv)	1.0	0.8	1.0
I_-(amp)	0 .010	0.0065	0.0065
I_B(amp)	0.565	0.425	0.500
V_A(volt)	7.4	7.25	7.6
I_A(amp)	47	38	46
P_B(kw)	1.980	1.530	1.750
P_D(kw)	0.045	0.029	0.029
P_M(kw)	0.006	0.008	0
P_A(kw)	0.348	0.276	0.350
P_T(kw)	2.379	1.843	2.129
T(mlb)	12.6	9.6	11.1
P/T(kw/lb)	189	192	191
η_p(percent)	83	83	83.5
η_m(percent)	90	91	92
η_e(percent)	75	75.5	76.5
I_{sp}(sec)	6550	6700	6670
I_-/I_B(percent)	1.7	1.5	1.3
P_A/I_B(kev/ion)	0.614	0.649	0.700

The instabilities noted above may have been caused by bowing of the electrodes. At low power levels the screen electrode bows toward the accelerating electrode reducing the gap and voltage holding capability of the accelerator system. At intermediate power levels of engine operation, the copper accelerating bowed out also but then cooled and repositioned. The long period instabilities noted are believed to be due to thermo-mechanical bowing and relaxation of the electrode. At higher engine power levels, the electrode bowing was apparently stabilized with the gap near normal. The use of materials with high coefficients of thermal expansion (such as iron for the screen electrode) will necessitate design modifications of the electrode mounting structure.

With the feasibility established of using permanent magnets on an electron bombardment cesium ion engine a new engine will be designed, fabricated, and tested. The freedom of design allowed by the elimination of the magnet coils should result in an overall reduction of engine weight. The weight of the present copper electromagnets is twice the weight of the permanent magnets used to perform the tests.

4. PLASMA DISTRIBUTION STUDIES

The DE engine operates with an average current density of about 4.5 ma/cm^2 over the entire source or about 9 ma/cm^2 averaged over the area of the apertures in the screen electrode. However, due to the plasma density distribution, this current is not uniform over the source area. At high thrust and performance levels the current density at the center of the electrode system is about 50 percent greater than the average density. If the neutral density in the accelerating gap is assumed to be uniform, this means that the erosion rate of the central portion of the accelerating electrode would be 50 percent greater than the average erosion rate.

This estimate is based on the assumption that the erosion is due primarily to charge exchange ions and not to directly intercepted ions. The only noticeable erosion of the accelerating electrodes of DE engines to date has occurred entirely on the exhaust side and is considered

to be due to charge exchange erosion.

4.1 Neutral Efflux

To learn more about the neutral distribution in the beam and to aid understanding of the operation of the arc discharge, a moveable neutral cesium detector was mounted in the vacuum system. This detector was located at an angle of 45 degrees to the beam axis and could be moved in such a way as to scan across a diameter of the engine. A schematic of the experimental set-up is shown in Figure 8.

An electrical readout from the detector positioning mechanism allowed the measured efflux to be plotted as a function of detector position directly on an X-Y recorder. A shutter was provided to allow determination of background signal levels from the neutral detector.

Initial tests made with a DE type electrode system gave uncertain results because of higher collimation of neutrals by the smaller apertures in the center of the electrodes. A set of uniform electrodes from the DD engine (EOS Report 3670-Final) was adapted to the DE engine to obtain more straightforward results.

Figure 9 presents data taken for operation with a 4 kv, 300 ma beam with 91 percent mass utilization. With the beam being extracted, there was a distinct dip in the neutral efflux from the center of the source. With the high voltage turned off but the arc left on, the plasma extrudes through the electrodes and the distribution is as shown in the middle curve of the figure. The detector signal is, of course, much larger in this case. The plasma extrudes most in the center giving rise to the peak at that position. With the feedrate maintained but the arc extinguished the third distribution was obtained.

4.2 Effect of Magnetic Field

Figure 10 shows the effect of the magnetic field on the neutral efflux distribution. The lower neutral efflux at higher fields somewhat obscures the fact that the dip in the center is more pronounced at higher magnetic fields. At zero magnetic field there was no dip and the neutral

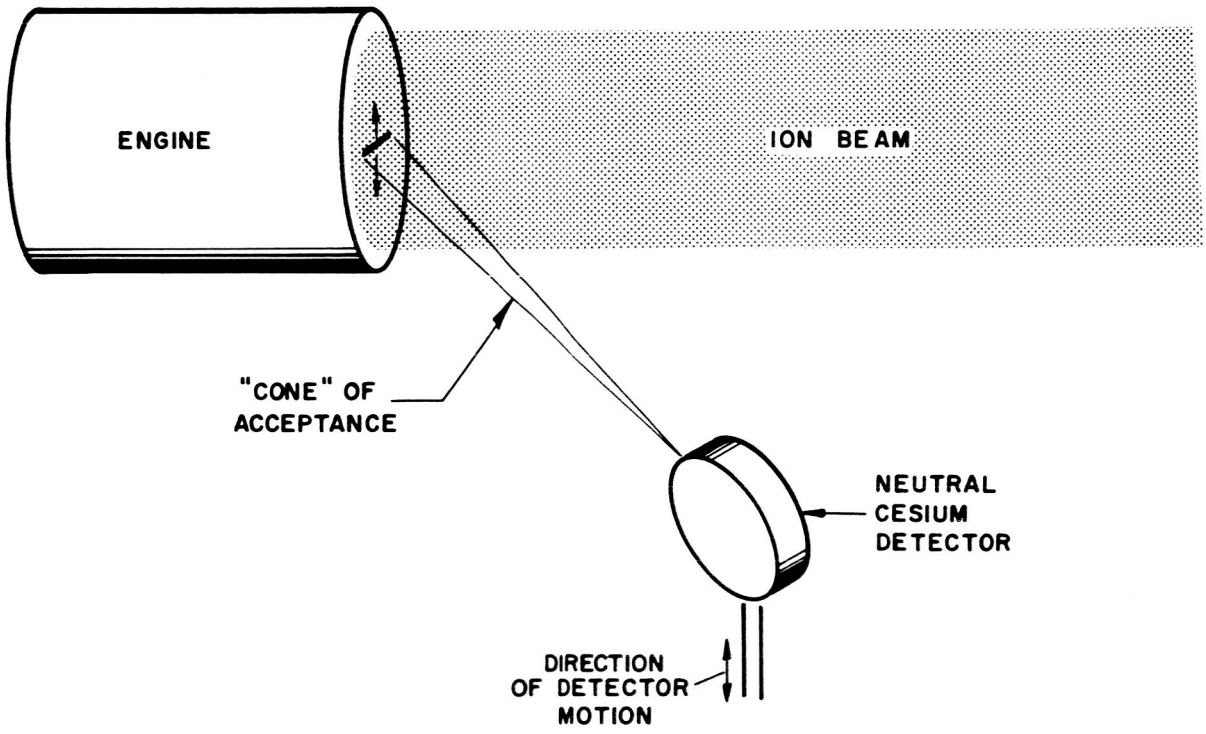

FIG. 8 SCHEMATIC OF SCANNING NEUTRAL DETECTOR EXPERIMENT

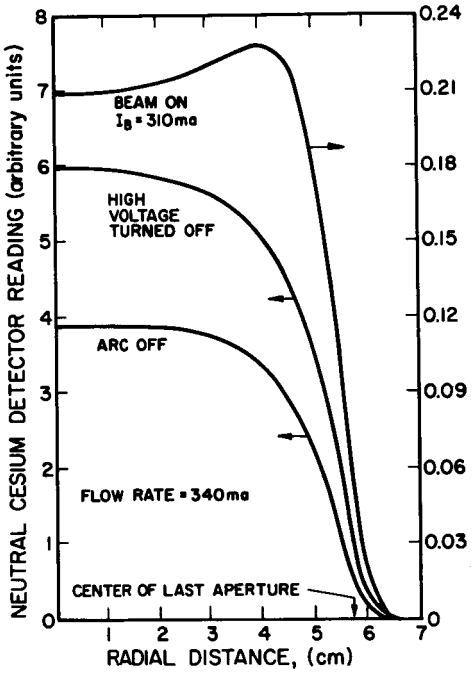

FIG. 9

VARIATION OF NEUTRAL EFFLUX DISTRIBUTION WITH BEAM ON, BEAM OFF, AND ARC OFF CONDITIONS

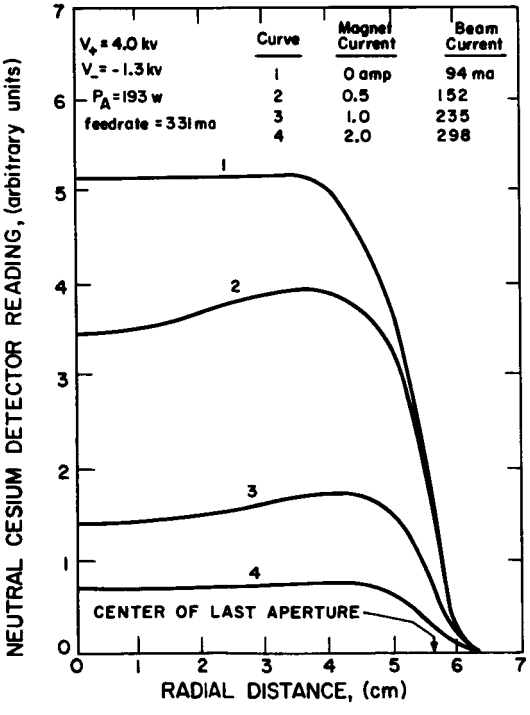

FIG. 10

NEUTRAL EFFLUX DISTRIBUTION WITH VARIED MAGNETIC FIELD

efflux distribution appeared to be quite similar to that for the case where the arc is extinguished. These results are consistent with theoretical considerations of the effect of the magnetic field on the plasma density distribution. For higher fields, the plasma density is more peaked at the center and the probability of a neutral atom being ionized is therefore higher in that region.

The acceptance angle was reduced on the neutral detector to provide higher resolution in the neutral efflux distributions. A Faraday cup collector was mounted alongside the neutral detector, extending into the center of the beam. A set of beam density profiles for a constant beam current of 300 ma at different values of magnet current appears in Figure 11. The peaking effect of the magnetic field is clearly shown, The large acceptance angle of this probe and the distance (about 5 inches) from the engine made it somewhat insensitive to changes in engine operation.

Further data were obtained with the neutral detector. Figure 12 shows neutral efflux profiles obtained at the same time as the beam profiles of Figure 11. A neutral detector mounted in the tank at a greater distance and with a larger acceptance angle gave the relative readings shown while these curves were taken. The difference in height of these curves is probably due to angular variations in engine efflux. At high magnetic fields the peak in efflux from the periphery of the engine becomes more pronounced. This peak may be due, in part, to evaporation of cesium from the anode.

4.3 Effect of Cathode Orifice

Figure 13 shows neutral efflux distributions obtained with three different cathode orifice configurations. These curves were taken with the same values of magnet current, beam current, and source potential. The arc power supply setting was held constant but arc power varied due to changes in arc impedance caused by the orifice changes.

Curve A was obtained with the standard orifice. Curve B was obtained with an orifice plate which had eight apertures equally

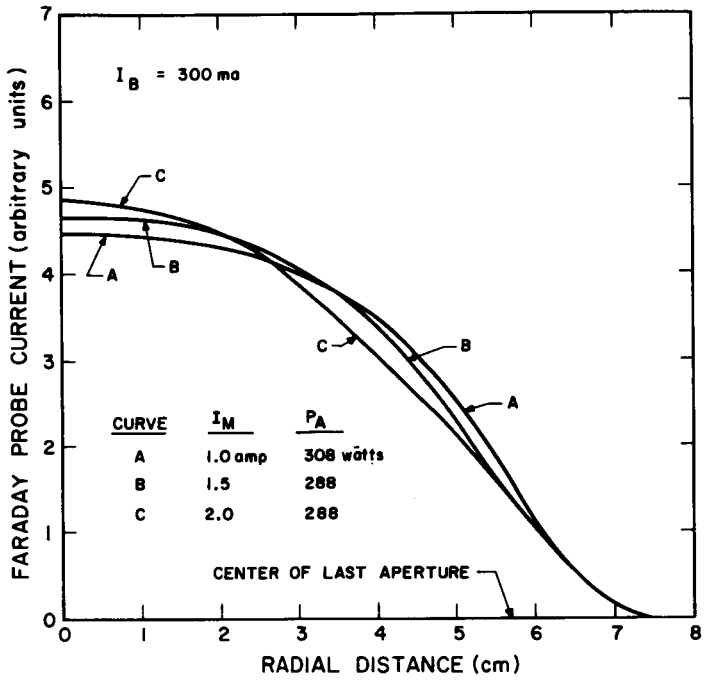

FIG. 11

BEAM DENSITY DISTRIBUTION VARIATIONS WITH MAGNETIC FIELD

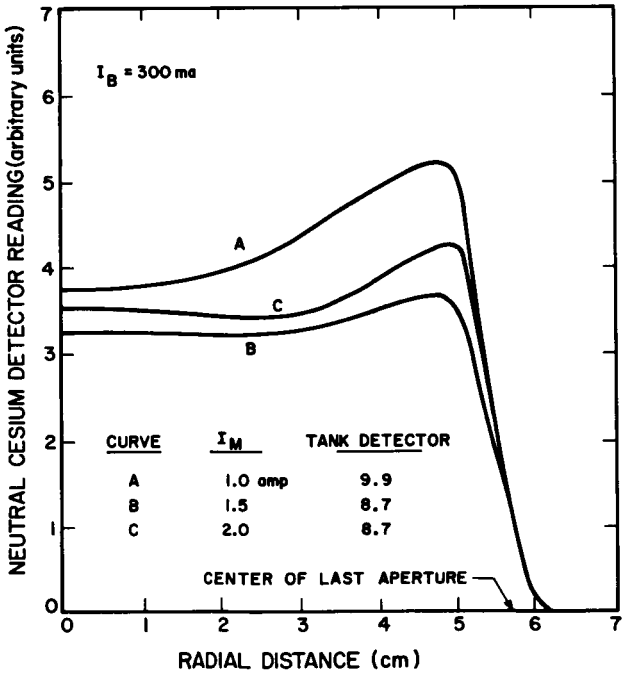

FIG. 12

NEUTRAL EFFLUX DISTRIBUTION VARIATION WITH MAGNETIC FIELD

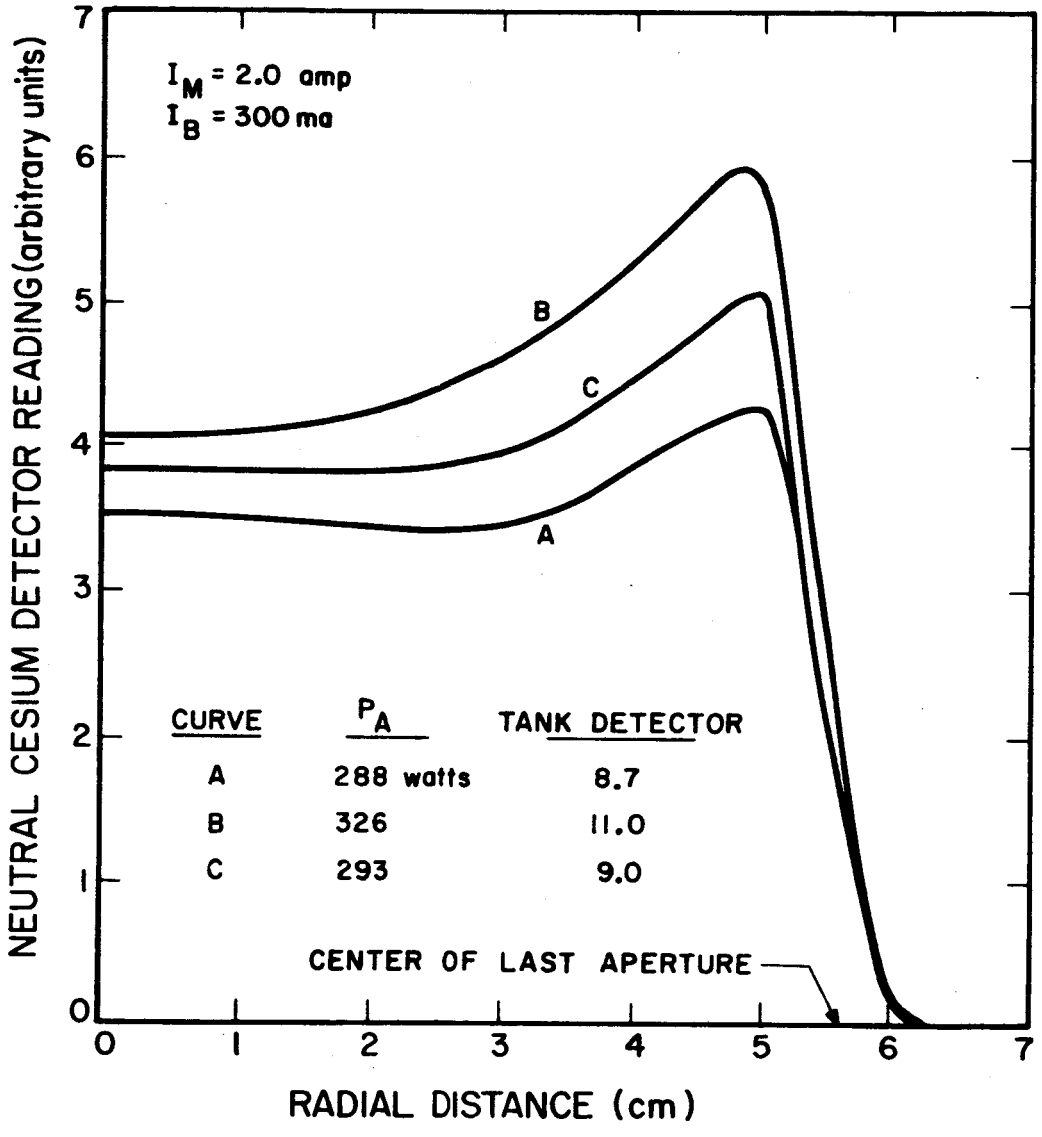

FIG. 13 NEUTRAL EFFLUX DISTRIBUTIONS WITH DIFFERENT CATHODE ORIFICE CONFIGURATIONS

spaced on a 1-3/4 inch diameter circle. The object of this test was to inject the electrons and cesium into the arc chamber to increase the ion density near the periphery of the electrodes. Beam profiles obtained showed questionable differences but the shape of curve B indicates an increase in the neutral density towards the edge of the chamber.

To obtain curve C, the original orifice was spaced away from the cathode to allow neutrals to enter the chamber radially. The effective cross sectional area of the resultant gap was approximately equal to the area of the central orifice. Here again a slight increase in neutral efflux distribution towards the periphery but no change in the beam density distribution was found.

Tests will be continued with the aid of a Faraday probe which has a smaller acceptance angle or mounted closer to the engine and a new neutral detector outlined below.

Since an uncertainty exists as to the angular variations in neutral efflux, a detector has been designed to work in the beam. Previous attempts to do this have failed due to high background levels and failure to sweep out all incoming ions.

The new detector will have a much more effective sweep system (longer sweep length and improved venting) and will use LN_2 cooling to condense cesium out of the filament housing. This detector will be placed in fabrication in June.

5. AUTOCATHODE IMPROVEMENT STUDIES

The present DE autocathode uses 90 watts of power from an internal heater to heat the emitter surface prior to establishing an arc. Studies are being performed to find ways to reduce or eliminate the starting power requirements, to simplify the construction of the cathode, and to generally improve autocathode start-up and operating characteristics.

5.1 Orifice Diameter

In order to investigate the effect of the cathode orifice, a series of orifice plates with varying aperture diameters was prepared.

Three of these orifices were operated in a DE engine with the following results.

The first orifice, as the control, had the standard 0.189 inch diameter. The data on source efficiency obtained with this orifice is shown by the circled points in Figure 14. This data is within one percent of the data found previously with the DE engines.

The second orifice tested had a diameter of 0.128 inches. (approximately two-thirds standard). Source efficiency was about two to three percent below that of the control as indicated by the triangles in Figure 14. This reduced cathode orifice made the arc more difficult to start; the cathode temperature had to be raised somewhat higher to initiate the discharge. The arc impedance was increased slightly and the orifice plate operated hot enough to cause an apparent recrystalization of the titanium at the orifice. Deterioration of this aperture over a long period of operation could cause the arc impedance to drift towards the normal levels.

The third orifice operated had a diameter of 0.284 inches (three-halves standard). This also reduced source efficiency by two to three percent. Starting characteristics were enhanced slightly (smoother turn-on) and the orifice ran cooler than normal as evidenced by an accumulation of backsputtered copper on the orifice. This orifice again appeared to reduce the arc impedance as compared with the control but insufficient data were obtained in this case. Arc instabilities were found when arc voltages above 9 volts were used during the engine heating phase of the turn-on sequence.

5.2 Autocathode Starting Temperature

To determine the minimum starting cathode temperature to initiate a discharge, an external heater was added to a DE cathode housing. With the heat source on the outside of the cathode, the internal temperature could be approximated by the housing wall temperature. Initial operation indicated that the arc could be initiated by maintaining the housing at a temperature high enough to prevent cesium condensation.

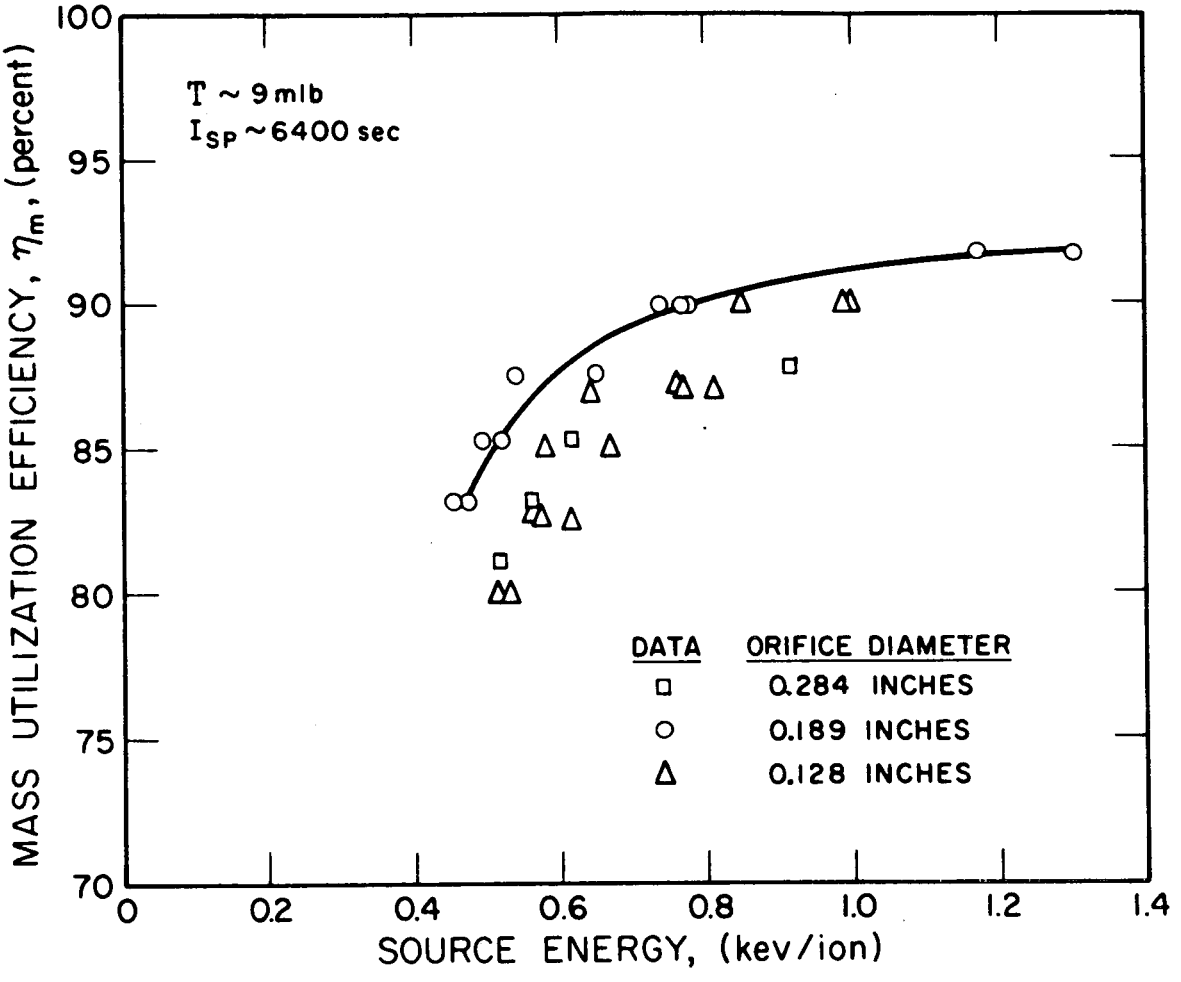

FIG. 14 EFFECT OF ORIFICE DIAMETER ON SOURCE EFFICIENCY

It appears that under these conditions enough cesium is delivered into the discharge chamber to initiate a glow discharge which develops into the full arc mode with autocathode operation.

Figure 15 shows a temperature time profile for a cold cathode startup. The internal cathode heater was not used. A power of 90 watts was applied through the external heater on the cathode housing until the arc was initiated. This test was made with a laboratory reservoir which has higher temperature and power requirements and longer response times than the zero-g type feed system.

For the first 20 minutes, the valve and cathode housings were brought to operating temperatures. No power was fed to the reservoir but some increase in reservoir temperature was observed due to heat conduction from the valve. At the end of the first heating phase, the reservoir power was turned on and after about 9 minutes, traces of cesium flow from the engine were observed with the neutral cesium detector in the vacuum tank. Three minutes later the arc started and increased to 30 amps and the reservoir power was regulated to maintain this value. During the first two minutes of arc operation the external heater was left on. When the arc current reached 20 amperes the heater was turned off and the cathode housing cooled to 300°C.

The thermocouple used to measure the cathode housing temperature was moved to a more accurate location and tests were continued to determine the minimum housing temperature required to start the discharge. A temperature of 340° to 350°C was found necessary when heating the cathode externally.

Using the internal heater it was possible to start consistently with a power of 25 watts for the normal orifice. During these starts, the housing reached a temperature of 240°C. The cathode heater, however, attained higher temperatures.

5.3 Externally Heated Cathode

A new cathode was designed for the DE engine which uses only an external heater. This cathode is shown in Figure 16a. The internally

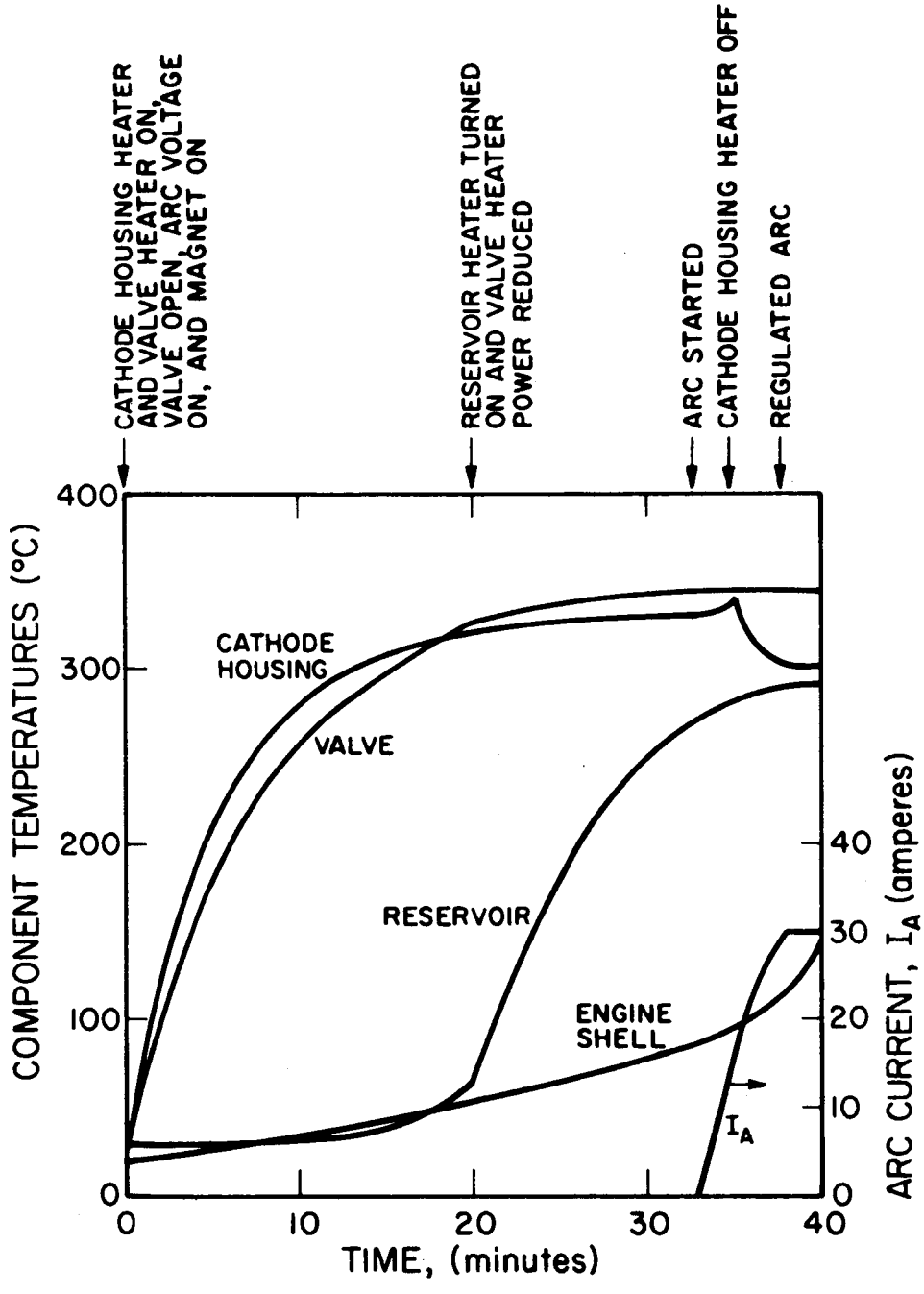

FIG. 15 COLD CATHODE START-UP PROFILE

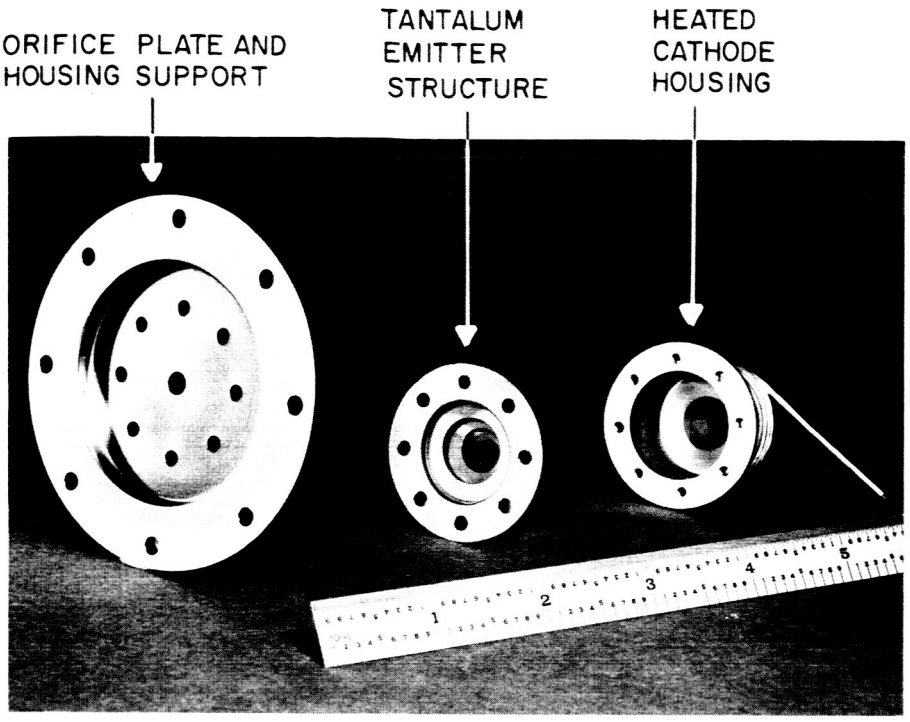

FIG. 16a EXTERNALLY HEATED CATHODE

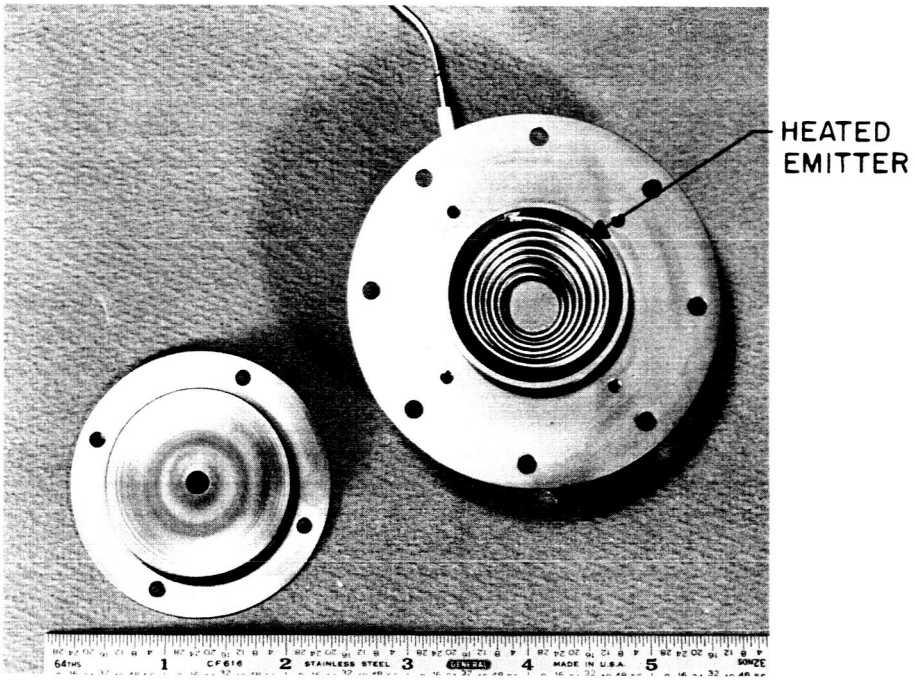

FIG. 16b INTERNALLY HEATED DE CATHODE WITH
ORIFICE PLATE REMOVED

heated cathode is shown for comparison in Figure 16b. The cathode is supported by the orifice plate in this design to reduce conductive cooling to the engine body. External surface area and thermal mass have been reduced but the volume and emitter area approximate those of the DE cathode. The emitter is formed from tantalum and is replaceable.

The arc was extremely difficult to start with this cathode. Once in operation, however, engine performance appeared normal. In order to start the arc a high voltage was first applied to the anode to start a glow discharge. It was more difficult to start with a cold engine shell than when the engine was near operating temperatures. It appears that a certain balance between the pressures in the arc chamber and the pressure in the cathode is necessary for starting. The starting characteristics of various autocathode configurations will be investigated further.

6. QUALITY ASSURANCE

At the beginning of the quarter, EOS Report 4920-QAP-1, "Inspection and Test Plan", was prepared and submitted to NASA-Lewis. This plan provides the planning function for inspections and tests to be conducted during the contract effort. Included in the test plan are the equipment log and failure report formats.

The plan was reviewed by the NASA-Lewis Office of Reliability and Quality Assurance. Provisions for extracting system data were clarified. EOS Form 73611509, "W.A. 4920 Failure Report", was revised in accordance with NASA-Lewis comment.

Shop traveller activity during the first quarter was primarily conerned with DER-1 engine and zero-gravity feed system support. Equipment logs were issued for the DER-1 engine, the zero-gravity feed system, and the government furnished control system. Two standing assembly requests, one each for the engine and feed system, were initiated. Both of these requests are still active.

Test procedure 4922-1, "Reliability Engine Component Weights", was released during the report period.

7. PLANS FOR NEXT QUARTER

During the next quarter DER-1 engine tests will be continued with molybdenum parts replacing the titanium alloy in the autocathode. A light weight permanent magnet engine will be designed, fabricated, and tested. The collimated faraday cup and the liquid nitrogen cooled neutral detector will be used in further analysis of engine configurations. The effect of the anode configuration as well as the cesium and electron injection system on the ion and neutral efflux distributions will be investigated.

To further understand the autocathode operation, temperature measurements on the cathode emitter will be made. Investigations will be made to determine the causes for different starting characteristics between the internally heated and externally heated cathodes and the effects of the magnetic and electric fields as well as internal pressures will be investigated.

DISTRIBUTION LIST

QUARTERLY PROGRESS REPORTS

CONTRACT NAS3-5250

	Addressee	Number of Copies
1.	NASA-Lewis Research Center 21000 Brookpark Road Cleveland, Ohio 44135 Attention: Spacecraft Technology Proc. Section	1
2.	NASA-Lewis Research Center 21000 Brookpark Road Cleveland, Ohio 44135 Attention: Technology Utilization Office	1
3.	NASA Headquarters FOB - 10B 600 Independence Avenue, Northeast Washington, D. C. 20546 Attention: RNT/James Lazar	2
4.	NASA Headquarters FOB - 10B 600 Independence Avenue, Northeast Washington, D. C. 20546 Attention: RRP.K. H. Thom	1
5.	NASA-Marshall Space Flight Center Huntsville, Alabama Attention: Dr. E. Stuhlinger	1
6.	Aeronautical Systems Division Wright-Patterson Air Force Base, Ohio Attention: AFAPL (APIE)/Lt. Robert Supp	1
7.	NASA-Lewis Research Center Electric Propulsion Laboratory 21000 Brookpark Road Cleveland, Ohio 44135 Attention: W. R. Mickelsen	1
8.	NASA-Lewis Research Center Electric Propulsion Laboratory 21000 Brookpark Road Cleveland, Ohio 44135 Attention: W. E. Moeckel	1
9.	NASA-Lewis Research Center Spacecraft Technology Division 21000 Brookpark Road Cleveland, Ohio 44135 Attention: J. H. Childs	2

	Addressee	Number of Copies
10.	NASA-Lewis Research Center Spacecraft Technology Division 21000 Brookpark Road Cleveland, Ohio 44135 Attention: R. Shattuck	1
11.	NASA-Lewis Research Center Spacecraft Technology Division 21000 Brookpark Road Cleveland, Ohio 44135 Attention: D. Lockwood	1
12.	NASA-Lewis Research Center Spacecraft Technology Division 21000 Brookpark Road Cleveland, Ohio 44135 Attention: James Wolters	8
13.	NASA-Lewis Research Center 21000 Brookpark Road Cleveland, Ohio 44135 Attention: Technical Information Division	1
14.	Jet Propulsion Laboratory 4800 Oak Grove Drive Pasadena, California 91103 Attention: John Paulson	1
15.	Detachment 4, ASR (ASQWR) Eglin Air Force Base, Florida Attention: Lt. C. F. Ellis	1
16.	Aerospace Corporation P. O. Box 95085 Los Angeles, California 90045 Attention: Library Technical Documents Group	1
17.	General Electric Company Flight Propulsion Laboratory Evandale, Ohio Attention: M. L. Bromberg	1
18.	Westinghouse Astronuclear Laboratories Electrical Propulsion Laboratory Pittsburgh, Pennsylvania 15234 Attention: H. W. Szymanowski	1
19.	Hughes Research Laboratories Malibu, California Attention: C. Brewer	1

	Addressee	Number of Copies
20.	TAPCO-Division of Thompson Ramo-Wooldridge, Inc. 7209 Platt Avenue Cleveland, Ohio 44104 Attention: R. T. Craig	1
21.	United Aircraft Corporation Research Department East Hartford, Connecticut Attention: R. C. Meyerand, Jr.	1
22.	Space Technology Laboratories 8433 Fallbrook Avenue Canoga Park, California Attention: Dr. Langmuir	1
23.	Aerojet-General Nucleonics Division San Ramon, California Attention: Mr. J. S. Luce	1
24.	NASA-Lewis Research Center 21000 Brookpark Road Cleveland, Ohio 44135 Attention: Library	2
25.	Ion Physics Corporation Burlington, Massachusetts Attention: Dr. S. V. Nablo	1
26.	NASA Scientific and Technical Information Facility Box 5700 Bethesda, Maryland 20014 Attention: RQT-2448/NASA Representative	6*
27.	North American Aviation, Inc. Technical Information Center 12214 Lakewood Avenue Downey, California Attention: Dept. 4-096-314	

*NOTE: The six (6) copies for the Scientific and Technical Information Center shall be sent to James Wolters, Lewis Research Center Project Manager. After review, they shall be forwarded to the Facility for reproduction and distribution as a NASA Contractor Report, high-number series.